


**ORIGINAL ARTICLE**

# Effects of different fluid management on lung and kidney during pressure-controlled and pressure-support ventilation in experimental acute lung injury

Eduardo Butturini de Carvalho<sup>1,2</sup> | Ana Carolina Fernandes Fonseca<sup>1</sup> |  
Raquel Ferreira Magalhães<sup>1</sup> | Eliete Ferreira Pinto<sup>1</sup> | Cynthia dos Santos Samary<sup>1</sup> |  
Mariana Alves Antunes<sup>1</sup> | Camila Machado Baldavira<sup>3</sup> |  
Lizandre Keren Ramos da Silveira<sup>3</sup> | Walcy Rosolia Teodoro<sup>3</sup> |  
Marcelo Gama de Abreu<sup>4,5,6</sup> | Vera Luiza Capelozzi<sup>3</sup> | Nathane Santanna Felix<sup>1</sup> |  
Paolo Pelosi<sup>7,8</sup> | Patrícia Rieken Macêdo Rocco<sup>1</sup> | Pedro Leme Silva<sup>1</sup> 

<sup>1</sup>Laboratory of Pulmonary Investigation, Institute of Biophysics Carlos Chagas Filho, Federal University of Rio de Janeiro, Rio de Janeiro, RJ, Brazil

<sup>2</sup>University of Vassouras, Vassouras, RJ, Brazil

<sup>3</sup>Department of Pathology, School of Medicine, University of São Paulo, São Paulo, Brazil

<sup>4</sup>Pulmonary Engineering Group, Department of Anaesthesiology and Intensive Care Therapy, Technische Universität Dresden, University Hospital Carl Gustav Carus, Dresden, Germany

<sup>5</sup>Department of Intensive Care and Resuscitation, Anesthesiology Institute, Cleveland Clinic, Cleveland, Ohio, USA

<sup>6</sup>Department of Outcomes Research, Anesthesiology Institute, Cleveland Clinic, Cleveland, Ohio, USA

<sup>7</sup>Department of Surgical Sciences and Integrated Diagnostics, University of Genoa, Genoa, Italy

<sup>8</sup>Anesthesia and Critical Care, San Martino Policlinico Hospital, IRCCS for Oncology and Neurosciences, Genoa, Italy

**Correspondence**

Pedro Leme Silva, Laboratory of Pulmonary Investigation, Institute of Biophysics Carlos Chagas Filho, Federal University of Rio de Janeiro, Centro de Ciências da Saúde, Avenida Carlos Chagas Filho, s/n, Bloco G-014, Ilha do Fundão, Rio de Janeiro, RJ 21941-902, Brazil.

Email: [pedroleme@biof.ufrj.br](mailto:pedroleme@biof.ufrj.br)

**Funding information**

Conselho Nacional de Desenvolvimento Científico e Tecnológico, Grant/Award Number: 483005/2020-6; Coordenação de Aperfeiçoamento de Pessoal de Nível Superior; Department of Science and Technology - Brazilian Ministry of Health; Fundação Carlos Chagas Filho de Amparo à Pesquisa do Estado do

**Abstract**

Optimal fluid management is critical during mechanical ventilation to mitigate lung damage. Under normovolemia and protective ventilation, pulmonary tensile stress during pressure-support ventilation (PSV) results in comparable lung protection to compressive stress during pressure-controlled ventilation (PCV) in experimental acute lung injury (ALI). It is not yet known whether tensile stress can lead to comparable protection to compressive stress in ALI under a liberal fluid strategy (LF). A conservative fluid strategy (CF) was compared with LF during PSV and PCV on lungs and kidneys in an established model of ALI. Twenty-eight male Wistar rats received endotoxin intratracheally. After 24h, they were treated with CF (minimum volume of Ringer's lactate to maintain normovolemia and mean arterial pressure  $\geq 70$  mmHg) or LF (~4 times higher than CF) combined with PSV or PCV ( $V_T = 6$  ml/kg, PEEP = 3 cmH<sub>2</sub>O) for 1 h. Nonventilated

Patrícia Rieken Macêdo Rocco and Pedro Leme Silva share senior authorship.

This is an open access article under the terms of the [Creative Commons Attribution](https://creativecommons.org/licenses/by/4.0/) License, which permits use, distribution and reproduction in any medium, provided the original work is properly cited.

© 2022 The Authors. *Physiological Reports* published by Wiley Periodicals LLC on behalf of The Physiological Society and the American Physiological Society.

Rio de Janeiro; Fundação de Amparo à Pesquisa do Estado de São Paulo, Grant/Award Number: 2018/20403-6 and 2019/12151-367 0

animals ( $n = 4$ ) were used for molecular biology analyses. CF-PSV compared with LF-PSV: (1) decreased the diffuse alveolar damage score (10 [7.8–12] vs. 25 [23–31.5],  $p = 0.006$ ), mainly due to edema in axial and alveolar parenchyma; (2) increased birefringence for occludin and claudin-4 in lung tissue and expression of zonula-occludens-1 and metalloproteinase-9 in lung. LF compared with CF reduced neutrophil gelatinase-associated lipocalin and interleukin-6 expression in the kidneys in PSV and PCV. In conclusion, CF compared with LF combined with PSV yielded less lung epithelial cell damage in the current model of ALI. However, LF compared with CF resulted in less kidney injury markers, regardless of the ventilatory strategy.

#### KEYWORDS

acute lung injury, fluid therapy, hemodynamics, immunofluorescence, immunohistochemistry, molecular biology, pressure-support ventilation

## 1 | INTRODUCTION

Ventilatory support and fluid therapy are cornerstones during the management of acute lung injury (ALI) (Cruz et al., 2018; Vieillard-Baron et al., 2016). Respiratory insufficiency requires the implementation of mechanical ventilation (MV), which in turn may worsen ventilator-induced lung injury (VILI). Overall, 60% of critically ill patients are also hemodynamically unstable, often requiring a high intake of intravenous fluids to restore tissue perfusion (Cruz et al., 2018; Gattinoni et al., 2010; Huppert et al., 2019; Marini & Rocco, 2020; Mekontso Dessap et al., 2016). However, little is known concerning interactions between fluids and the ventilatory strategy.

Assisted spontaneous ventilation can reduce VILI compared with controlled MV in preclinical (Magalhães et al., 2018; Pinto et al., 2020; Saddy et al., 2010) and clinical (van Haren et al., 2019) studies; the latter show increased ventilation-free days and fewer days in the intensive care unit (Saddy et al., 2010, 2013; Santos et al., 2017; van Haren et al., 2019). However, due to cardiopulmonary interaction, assisted spontaneous breathing can increase lung perfusion (due to higher right ventricle preload and lower afterload) and transvascular filtration pressure, both of which may worsen lung edema (Vieillard-Baron et al., 2016; Yoshida et al., 2017). In addition, lung edema may increase further if tight junction connections, as occludin, which are constitutive in epithelial and endothelial structural cells, are lost during the stretch movements (Cavanaugh Jr et al., 2001). During assisted spontaneous ventilation such as pressure-support ventilation (PSV), pleural pressure decreases, leading to tensile stress (Silva et al., 2022), whereas during pressure-controlled ventilation (PCV), a positive increase in pleural pressure is observed, resulting in compressive stress (Silva & de Abreu, 2018). The difference between tensile and

compressive stresses has been studied both in vitro (Bachofen et al., 1987; Tschumperlin et al., 2000) and in vivo (Roan & Waters, 2011). Under normovolemia and protective ventilation, tensile stress in the lung during PSV leads to comparable pulmonary protection to compressive stress during PCV in experimental ALI (Pinto et al., 2020). We hypothesized that the tensile stress during PSV would be protective under conservative fluid (CF) strategy, as compared to compressive stress during PCV, but not under a liberal fluid strategy (LF). We compared the interaction of CF and LF during PSV and PCV on lungs and kidneys in an established ALI model.

## 2 | MATERIALS AND METHODS

### 2.1 | Study approval

This study was approved by the Animal Care and Use Committee (CEUA: 038–18) of the Health Sciences Center, Federal University of Rio de Janeiro. All animals were treated in compliance with the *Principles of Laboratory Animal Care* by the National Society for Medical Research and the US National Academy of Sciences *Guide for the Care and Use of Laboratory Animals*. The current study followed the guidelines of the *Animal Research: Reporting of In Vivo Experiments* (Percie du Sert et al., 2020). Conventional animals were housed at a controlled temperature (23°C) in a controlled light–dark cycle (12–12 h), with free access to water and food.

### 2.2 | Animal preparation

Beginning at 8:00 a.m., 28 male Wistar rats (body weight,  $389 \pm 40$  g, 10–12 weeks old) were anesthetized

consecutively by inhalation of isoflurane 1.5%–2.0% (Isoforine; Cristália) during spontaneous breathing and underwent intratracheal instillation of *Escherichia coli* lipopolysaccharide (LPS,  $9.6 \times 10^6$  endotoxin units/ml) (Merck Millipore), suspended in 0.9% saline solution (total volume 200  $\mu$ l) to induce ALI (Magalhães et al., 2018; Silva et al., 2013). After full recovery from anesthesia and a 24-h observation period, in the early morning (around 8:00 a.m.) the animals received diazepam (10 mg/kg) and ketamine (100 mg/kg, i.p.) intraperitoneally (i.p.), and tracheostomy was performed after local anesthesia (0.4 ml of 1% lidocaine) in the ventral neck midline. Anesthesia was maintained by a syringe pump (Digipump, Digicare Animal Health) delivering a constant rate infusion of ketamine and midazolam (50 and 2 mg/kg/h, respectively) intravenously (i.v.) through a tail vein catheter (Jelco 24G; Becton Dickinson). An 18G catheter (Arrow International) was inserted in the right internal carotid artery to measure continuous mean arterial pressure (MAP). The level of anesthesia was titrated according to MAP levels during experiment. Heart rate and body temperature were monitored continuously (LifeWindow 6000 V; Digicare Animal Health). Body temperature was maintained at  $37.5 \pm 1^\circ\text{C}$  with a heating bed (EFF 421, INSIGHT). Esophageal pressure ( $P_{\text{es}}$ ) was measured using a 30-cm water-filled catheter with side holes at the tip (PE205, Becton Dickinson) passed into the esophagus and connected to a pressure transducer (UT-PL-400; SCIREQ). Correct positioning was assessed by the occlusion test (Baydur et al., 1982). Four animals were subjected to intratracheal instillation of LPS and were used as nonventilated controls for molecular biology analyses after 24 h.

### 2.3 | Experimental protocol

After animal preparation, lungs were ventilated mechanically with Servo-i (MAQUET) via PCV or PSV (flow triggering) during which a researcher (E.B.C.) adjusted the driving pressure to  $V_T \approx 6 \text{ ml/kg}$  (PEEP = 3  $\text{cmH}_2\text{O}$  and  $\text{FiO}_2 = 0.4$ ). As PCV inherently requires neuromuscular blockade, animals in this group were paralyzed by intravenous administration of pancuronium bromide (1 mg/kg; Cristália). Pilot studies were performed in the CF strategy group to estimate the minimal amount of Ringer's lactate (B. Braun) required to maintain normovolemia (evaluated using echocardiography) and  $\text{MAP} \geq 70 \text{ mmHg}$  for 1 h in experimental ALI. The mean cumulative fluids infused in both the CF-PCV and CF-PSV groups were multiplied by 4 for the cumulative amount of fluid for LF; thus, the infusion rate was adjusted for the LF-PSV and LF-PCV groups for 1 h ( $n = 6$  per group). The pilot procedure did not hinder the randomization of the animals. The

study design and temporal evolution are summarized in Figure 1. At  $T_{60}$ , heparin was injected (1000 U i.v.), and the animals were euthanized by an intravenous overdose of sodium thiopental (60 mg/kg; Cristália). The trachea was clamped at PEEP = 3  $\text{cmH}_2\text{O}$ , and the lungs and kidneys were removed *en bloc* for histology and molecular biology analysis.

### 2.4 | Data acquisition and respiratory mechanics

Airflow, airway pressure ( $P_{\text{aw}}$ ), and esophageal pressure ( $P_{\text{es}}$ ) were recorded throughout the experiments by software written in LabView (National Instruments) (Wierzchon et al., 2017).  $V_T$  was calculated by digital integration of the airflow signal. Respiratory rate was calculated from swings in  $P_{\text{es}}$  as the frequency per minute of each type of breathing cycle. Transpulmonary pressure ( $P_L$ ) was calculated during inspiration and expiration as the difference between  $P_{\text{aw}}$  and  $P_{\text{es}}$ . Peak and plateau transpulmonary pressures ( $P_{\text{peak,L}}$  and  $P_{\text{plat,L}}$ ) were measured. To calculate the plateau pressures ( $P_{\text{plat}}$ ), the airways were occluded at end inspiration (zero airflow) for 3 s. Static transpulmonary driving pressure ( $\Delta P_{\text{Lstat}}$ ) was calculated at the end of inspiration (max) and expiration (min) as the difference between driving airway pressure ( $\Delta P_{\text{RS}}$ ) and the change in esophageal pressure ( $\Delta P_{\text{es}}$ ), according to the following equation (Bellani et al., 2016):  $\Delta P_L = \Delta P_{\text{RS}} - \Delta P_{\text{es}}$  where  $\Delta P_{\text{es}} = P_{\text{es,max}} - P_{\text{es,min}}$ .  $P_{\text{oes}_{0.1}}$  is the esophageal pressure measured at 100 ms of inspiration after occlusion at end expiration, which reflects the neuromuscular drive (Elliott et al., 1993). All signals were amplified in a 4-channel signal conditioner (SC-24; SCIREQ) and sampled at 200 Hz with a 12-bit analog-to-digital converter (National Instruments). All data were computed by a routine written in MATLAB (R2007a; MathWorks).

### 2.5 | Echocardiography

Transthoracic echocardiography was performed (UGEO HM70A, 8–13 MHz transducer; Samsung) at  $T_0$  and  $T_{60}$  according to the American Society of Echocardiography recommendations (Lang et al., 2015). The following M-mode, bidimensional, and pulsed Doppler DICOM images were captured and later analyzed in EchoPac (GE Healthcare): the diameter of the internal vena cava ( $\text{IVC}_d$ ), velocity-time integral (VTI), aortic valve diameter ( $\text{AV}_d$ ), and pulmonary acceleration to pulmonary ejection time ratio (PAT/PET). Left ventricle cardiac output ( $\text{CO}_{\text{LV}}$ ) was calculated as  $[(\text{AV}_d)^2 \times 0.785 \times (\text{VTI})] \times (\text{heart rate})$ ; variation in left ventricle stroke volume  $\text{SVV}_{\text{LV}}$  as  $(\text{SV}_{\text{max}} - \text{SV}_{\text{min}}) \times 100/$

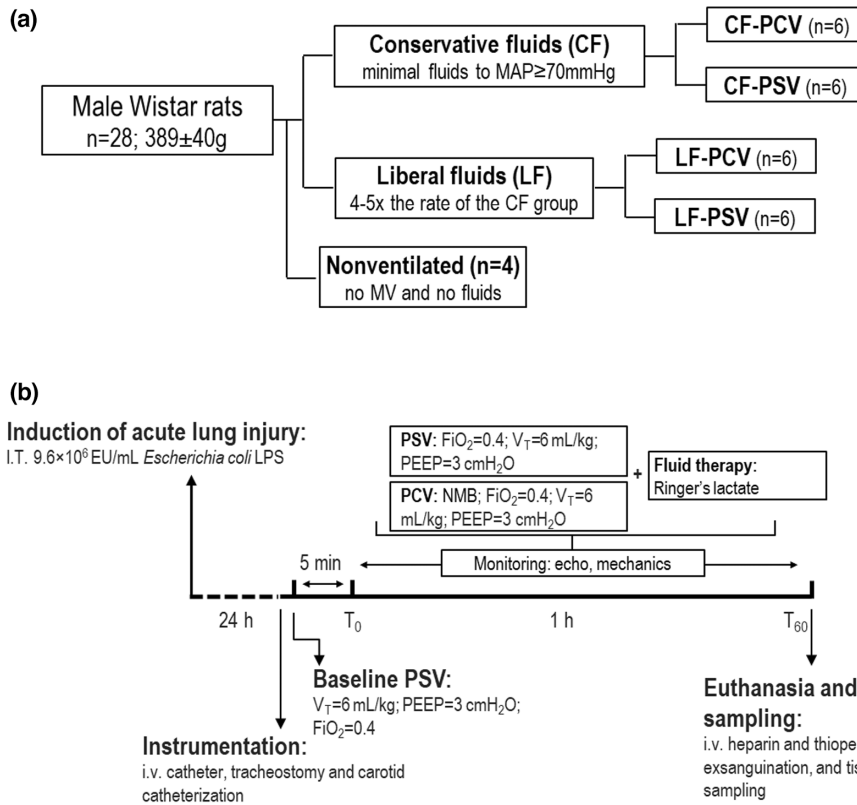


**FIGURE 1** Experimental design and temporal evolution. (a) Experimental design. The CF regimen was defined as the minimal amount of Ringer's lactate to maintain mean arterial pressure (MAP)  $\geq 70$  mmHg. The LF regimen was defined as  $\sim 4$ – $5$  times higher fluids than in the CF groups. (b) Temporal evolution. CF, conservative fluid; Echo, echocardiography;  $\text{FiO}_2$ , inspired fraction of oxygen; i.v., intravenous; LF, liberal fluid; MV, mechanical ventilation; PEEP, positive end-expiratory pressure;  $V_T$ , tidal volume.

$[(\text{SV}_{\text{max}} + \text{SV}_{\text{min}})/2]$ ; and the vena cava collapsibility index (VCCI) as  $((\text{IVC}_{\text{dmax}} - \text{IVC}_{\text{dmin}}) \times 100 / \text{IVC}_{\text{dmin}})$ .

## 2.6 | Lung histology

### 2.6.1 | DAD score

All pathologists were blinded to the group assignment. To assess the diffuse alveolar damage (DAD) score, the left lung was embedded in paraffin after fixation in 4% formaldehyde. Sections were cut  $4 \mu\text{m}$  thick longitudinally from the central zone with a microtome and stained with hematoxylin-eosin (HE). The left lung was assessed in a light microscope (Olympus BX51; Olympus Latin America) for the DAD score by two independent investigators (A.C.F.F. and V.L.C.) blinded to group assignment. The scores of each expert were combined to yield a final score by arithmetic averaging (Kiss et al., 2016). The value of kappa was 0.82. Photomicrographs at magnifications of  $\times 100$ ,  $\times 200$ , and  $\times 400$  were obtained from 10 non-overlapping fields of view per section using a light microscope (Olympus BX51, Olympus Latin America). Briefly, scores of 0–4 were used to represent the severity of edema and inflammatory infiltrate in both axial and alveolar parenchyma, thus totaling four parameters (Uhlir et al., 2014). In addition, the extent of each scored characteristic per field of view was determined on a scale of

0–4, with 0 denoting no visible evidence and 4 denoting widespread involvement. Scores were calculated as the product of the severity and extent of each parameter on a range of 0–16. The cumulative DAD score was calculated as the sum of each parameter characteristic and ranged from 0 to 64.

### 2.6.2 | Quantification of heterogeneous airspace enlargement

Airspace enlargement was assessed by measuring the mean linear intercept between alveolar walls at a magnification of  $\times 400$ , as described elsewhere (Hsia et al., 2010). The central moment of the mean linear intercept ( $D_2$  of the mean linear intercept between the alveolar walls) was calculated from 20 airspace measurements (Parameswaran et al., 2006) using the following equation:

$$D_2 = \mu \cdot \left( 1 + \frac{\sigma^2}{\mu^2 + \sigma^2} \right) \cdot \left( 2 + \sigma \cdot \frac{\gamma}{\mu} \right)$$

where  $\mu$  is the mean,  $\sigma$  is the standard variation and  $\sigma^2$  is the variance in airspace diameter, and  $\gamma$  is the skewness of the diameter dispersion. The heterogeneity index, represented by  $\beta$ , was calculated by the ratio between  $D_2$  and the mean linear intercept between the alveolar walls (Wierzbicki et al., 2017).



### 2.6.3 | Quantification of perivascular edema

To quantify perivascular edema, 10 random, noncoincident microscopic fields containing vessels were evaluated. The number of points falling on areas of perivascular edema and the number of intercepts between the lines of the integrating eyepiece and the basal membrane of the vessels were counted. The interstitial perivascular edema index was calculated as follows: number of points<sup>0.5</sup>/number of intercepts (Cavalcanti et al., 2014; Santiago et al., 2010).

### 2.6.4 | Quantification of occludin by immunohistochemistry

The specimens for lung immunohistochemistry were obtained from the archived formalin-fixed paraffin-embedded lung histologic sections incubated with anti-occludin monoclonal antibody diluted in 50 parts of citrate (Santa Cruz sc-133256, Santa Cruz Biotechnology) and were placed in tissue microarrays from most representative areas previously marked in HE-stained slides. Occludin quantification was measured as the number of positive cells/mm<sup>2</sup> and performed using a semi-assisted method in QuPath (v0.2.1; Centre for Cancer Research & Cell Biology, Edinburgh University) as described previously (Balancin, Teodoro, Baldavira, et al., 2020; Balancin, Teodoro, Farhat, et al., 2020).

### 2.6.5 | Immunofluorescence of occludin and claudin-4

Immunofluorescence was performed on an immunofluorescence microscope (Olympus BX51, Olympus) for qualitative assessment of occludin and claudin-4 using the following antibodies: anti-occludin Santa Cruz (sc-133256, Santa Cruz Biotechnology), anti-vimentin (D21H3 XP mAb; Cell Signaling, Uniscience do Brasil), anti-claudin-4 (ab15104; Abcam), and anti-actin (M0851, Dako; Agilent Technologies Brasil) diluted 1:30; 1:100; 1:300, and 1:100 in citrate, respectively.

## 2.7 | Kidney histology

Two semi-quantitative score systems were used for kidney histology. Brush border analysis was performed in digital photos of 10 kidney regions from 400× magnified slides stained with periodic acid Schiff. Scores ranged from 0 to 4 according to the area affected by brush border loss, cell tumefaction, and interstitial edema (0, no evidence;

1, 1%–25%; 2, 25%–50%; 3, 50%–75%; 4, 75%–100%). The final score was the mean from 10 visual fields and ranged between 0 (no damage) to 4 (full involvement). The acute kidney injury (AKI) score was adapted from previous studies (Bateman et al., 2016; Hüter et al., 2009) and was measured in HE-stained kidney slides, ranging from 0% to 100%. Image-Pro Plus v.6.0.0.260 (Media Cybernetics) was used to calculate the percentage of the visual field corresponding to calibrated colors associated with edema. The results are presented as the mean of 10 visual fields. Semi-quantitative score was calculated by two expert investigators (A.C.F.F. and V.L.C.) blinded to group assignment.

## 2.8 | Molecular biology of lung and kidney

Quantitative real-time reverse transcription polymerase chain reaction (RT-qPCR) was performed on kidneys for kidney injury molecule 1, neutrophilic gelatinase-associated lipocalin (NGAL), and interleukin-6 (IL-6), and on lung tissue for zona occludens-1 (ZO-1) and metalloproteinase-9 (MMP-9). The primer sequences are shown in Table S1. Slices from the right superior lung lobe and right kidney were sampled in cryotubes and stored at –80°C after immersion in liquid nitrogen. Extraction of total RNA was achieved with an RNA total SV system (Promega). RNA concentration was measured using Nanodrop ND-1000 spectrophotometry. cDNA was synthesized and amplified from total RNA with a GoTaq 2-STEP RT-qPCR system (Promega). The RT-PCR reaction was performed with Applied Biosystems SYBR green PCR Master Mix (Thermo Fisher Scientific), and relative mRNA was measured using an SYBR green detection system (ABI 7500 Real-Time PCR; Applied Biosystems). For each sample, the expression of each gene was normalized to that of the housekeeping gene 36B4 (Akamine et al., 2007) and expressed as fold change relative to the nonventilated group, using the  $2^{-\Delta\Delta Ct}$  method, where  $\Delta Ct = Ct(\text{reference gene}) - Ct(\text{target gene})$ . All analyses were performed by M.A.A. who was blinded to the group assignment.

## 2.9 | Statistical analysis

Sample size was calculated using G\*Power 3.9.1.2 (Düsseldorf University, Düsseldorf, Germany) and the following settings: power ( $1 - \beta = 0.8$ ); significance level ( $\alpha = 0.05$ ); allocation ratio  $N2/N1 = 1$ ; effect size ( $d = 1.83$ ) according to the difference in the DAD score between PSV and PCV obtained from published data (Magalhães et al., 2018). Comparisons were made

between groups under the same ventilatory or fluid strategy (CF-PCV vs. CF-PSV; CF-PCV vs. LF-PCV; CF-PSV vs. LF-PSV; LF-PCV vs. LF-PSV). The primary outcome was the DAD score, and the secondary outcomes were alveolar heterogeneity, expression of occludin in lung tissue, as well as expression of claudin-4, vimentin, and  $\alpha$ -actin in lung tissue, and molecular biology data. Data were tested for normality by the Shapiro–Wilk test. Body weight, the alveolar heterogeneity index, AKI score, and brush border analysis were assessed by one-way ANOVA with Holm–Sidak multiple comparison tests. Fluid composition, respiratory mechanics, and hemodynamics were assessed by two-way ANOVA with Holm–Sidak multiple comparison tests. Fluid infusion rate, molecular biology data, perivascular edema, DAD score, and quantification of occludin were compared using the Kruskal–Wallis test followed by Dunn’s multiple comparison tests. Spearman correlation was calculated for MAP versus  $CO_{LV}$ , fluid infusion rate versus perivascular edema, fluid infusion rate versus DAD, and occludin versus DAD. Parametric data were expressed as the mean  $\pm$  SD and nonparametric data as the median (interquartile range). All tests were performed in GraphPad 9 (GraphPad Software).

### 3 | RESULTS

All animals survived to the end of the experiment, without any missing data. LF-PCV and LF-PSV received a total amount of fluid (median [interquartile range]) equal to

23.1 ml/kg/h (22.7–24.8) and 26.5 ml/kg/h (23.2–34.8), respectively; CF-PCV and CF-PSV received at total amount of fluid equal to 4.2 ml/kg/h (3.5–9.1) and 4.4 ml/kg/h (3.1–8.0), respectively, as shown in Figure S1.

No significant differences were observed in MAP and  $CO_{LV}$  among the groups.  $SVV_{LV}$  and VCCI were lower in the LF-PCV group at  $T_{60}$  compared with  $T_0$  ( $p = 0.023$  and  $p = 0.037$ , respectively), showing hypervolemia status (Table S2). All groups were protectively ventilated ( $V_T = 6$  ml/kg), and no difference in static  $\Delta P_L$  was found among the groups.  $P_{peak,L}$  and  $P_{plat,L}$  were higher in both PSV groups compared with the PCV groups, regardless of the fluid regimen (Table S3). No significant difference in  $Poes_{0.1}$  was observed between the CF-PSV and LF-PSV groups.

The alveolar heterogeneity index was similar among the groups (Table 1). The cumulative DAD score was lower with CF-PSV and LF-PCV than LF-PSV, mainly due to lower axial parenchyma and intra-alveolar parenchyma edema ( $p < 0.05$  for both) (Figure 2; Table 1). Axial parenchyma edema, intra-alveolar edema, and cumulative DAD score were positively correlated with the fluid infusion rate ( $r = 0.544$ ;  $r = 0.600$ , and  $r = 0.494$ , respectively, with  $p < 0.05$  for all three correlations) (Figure S2). The perivascular edema index was lower in both CF groups compared with the LF groups (CF-PCV vs. LF-PCV,  $p = 0.046$ ; CF-PSV vs. LF-PSV,  $p = 0.009$ ), and positively correlated with the fluid infusion rate ( $r = 0.424$ ,  $p = 0.039$ ). LF-PCV was associated with increased expression of occludin in lung tissue compared with LF-PSV ( $p = 0.026$ , Figure 2). The expression of occludin in lung tissue was negatively

**TABLE 1** Cumulative diffuse alveolar damage score and its components, alveolar heterogeneity index, and perivascular edema

	CF		LF	
	PCV	PSV	PCV	PSV
Axial parenchyma				
Edema (cuff) (0–16)	2 (1–4)	3 (1–4)	2 (2–2.5)	10 (7–12) <sup>#,†</sup>
Inflammatory infiltrate (0–16)	3.5 (3–6.8)	3 (1.75–4)	4 (3.8–4.5)	3 (2–4)
Alveolar parenchyma				
Edema intra-alveolar (0–16)	3 (1–4)	1 (0–2)	1.5 (0.8–2.5)	10.5 (8–13) <sup>#,†</sup>
Inflammatory infiltrate (0–16)	3.5 (2.8–4)	4 (2–4)	2.5 (1–4)	3 (2–3.8)
Cumulative DAD score (0–64)	13 (10.3–15.8)	10 (7.8–12)	9 (7.8–11.3)	25 (23–31.5) <sup>#,†</sup>
$\beta$ ( $D_2/Lm$ )	1.29 (1.21–1.42)	1.26 (1.19–1.50)	1.32 (1.24–1.52)	1.20 (1.07–1.31)
Perivascular edema	0.62 (0.54–0.68)	0.57 (0.52–0.62)	0.83 (0.63–0.85) <sup>*</sup>	0.71 (0.64–0.84) <sup>#</sup>

*Note:* Values are presented as the median (interquartile range [25%–75%]) of 6 animals per group. Comparisons were performed by Kruskal–Wallis test followed by Dunn’s multiple comparison test ( $p < 0.05$ ).

Abbreviations: CF, conservative fluid therapy; DAD, diffuse alveolar damage; LF, liberal fluid therapy; PCV, pressure-controlled ventilation; PSV, pressure-support ventilation;  $\beta$ , alveolar heterogeneity index.

<sup>\*</sup> $p < 0.05$  significantly different from CF-PCV.

<sup>#</sup> $p < 0.05$  significantly different from CF-PSV.

<sup>†</sup> $p < 0.05$  significantly different from LF-PCV.

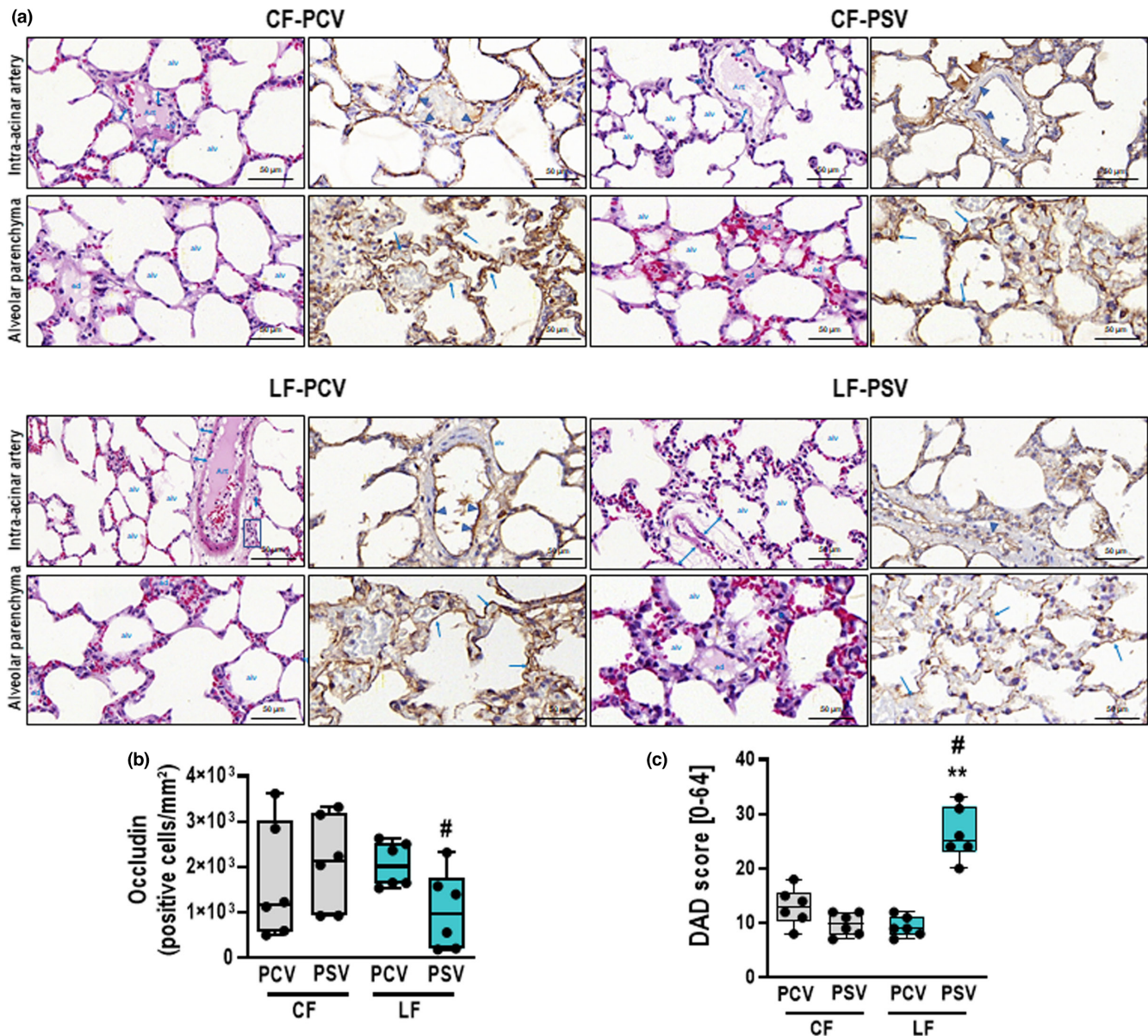


**FIGURE 2** DAD score and immunohistochemistry for occludin. (a) Representative images of histologic sections of alveolar pulmonary parenchyma (alveolar sacs and ducts, alveoli, and associated capillary loops) and perivascular sections (intra-acinar arteries) stained by hematoxylin-eosin and immunohistochemistry for occludin at high magnification. The intra-acinar artery sections of CF-PCV demonstrate discrete cuff-shaped perivascular edema (double blue arrowheads) coincident with prominent expression of occludin by the endothelial cells of the artery (blue arrowheads). A similar immunophenotypic pattern of occludin was found in CF-PSV and LF-PCV, except for slightly cuff-shaped perivascular edema (blue arrowheads) and mild inflammatory cells (blue square). In contrast, the LF-PSV alveolar parenchyma exhibited almost absence of occludin in the endothelium of capillary loops (blue arrows). (b) Boxplot of occludin quantification in lung tissue.  $p = 0.026$ . (c) DAD score. \*\*, means different from CF-PSV ( $p < 0.01$ ); #, vs LF-PCV ( $p < 0.05$ ). Alv, alveoli; art, artery; CF, conservative fluid therapy; DAD, diffuse alveolar damage; ed, edema; LF, liberal fluid therapy; PCV, pressure-controlled ventilation; PSV, pressure-support ventilation.

associated with axial and intra-alveolar parenchyma edema ( $r = -0.432$  and  $r = -0.438$ , respectively;  $p < 0.05$  for both correlations). Qualitative assessment of occludin and claudin-4 by immunofluorescence showed increased birefringence for the LF-PCV group compared with the LF-PSV group (Figure 3; Figure S3, respectively).

In lungs, ZO-1 gene expression was higher in the LF-PCV group than in the LF-PSV group ( $p = 0.041$ ) and

increased more in the LF-PCV group than in the CF-PCV group ( $p = 0.015$ ). MMP-9 expression was lower in the LF-PCV group than in the LF-PSV group ( $p = 0.026$ ) (Figure 4).

In kidneys, gene expressions of NGAL and IL-6 did not differ significantly between the LF-PSV and LF-PCV groups. NGAL expression was lower in the LF-PSV group than in the CF-PSV group ( $p = 0.021$ ). IL-6 expression was



reduced more in the LF-PCV group than in the CF-PCV group ( $p = 0.026$ ). In addition, no significant differences in AKI scores and brush border analysis were detected between the different groups (Table S3).

## 4 | DISCUSSION

In the present ALI model, we found that ALI compared with LF during pressure support ventilation: (1) the DAD score decreased more, mainly due to edema in axial and alveolar parenchyma; (2) birefringence for occludin and claudin-4 in lung tissue was increased; and (3) neutrophil gelatinase-associated lipocalin expression in kidney tissue increased more. Pressure support ventilation in

combination with CF, but not LF, promoted less lung epithelial damage in this model of ALI. However, the beneficial effects on kidney were observed in LF compared with ALI. Our data suggest that the fluid strategy should be strictly monitored during mechanical ventilation, mainly during pressure support ventilation.

We used a model of *E. coli* LPS induced-mild lung injury because it reproduces changes in lung function and histology (alveolar collapse, neutrophil infiltration, and edema) of human ARDS (Matute-Bello et al., 2011). A mean fluid infusion rate as low as 5.4 ml/kg/h (observed in the CF-PCV and CF-PSV groups) was sufficient to maintain MAP  $\geq 70$  mmHg and normal  $CO_{LV}$  (Watson et al., 2004) values in the CF groups, probably because intratracheal instillation of LPS, as opposed to sepsis-induced lung injury, does

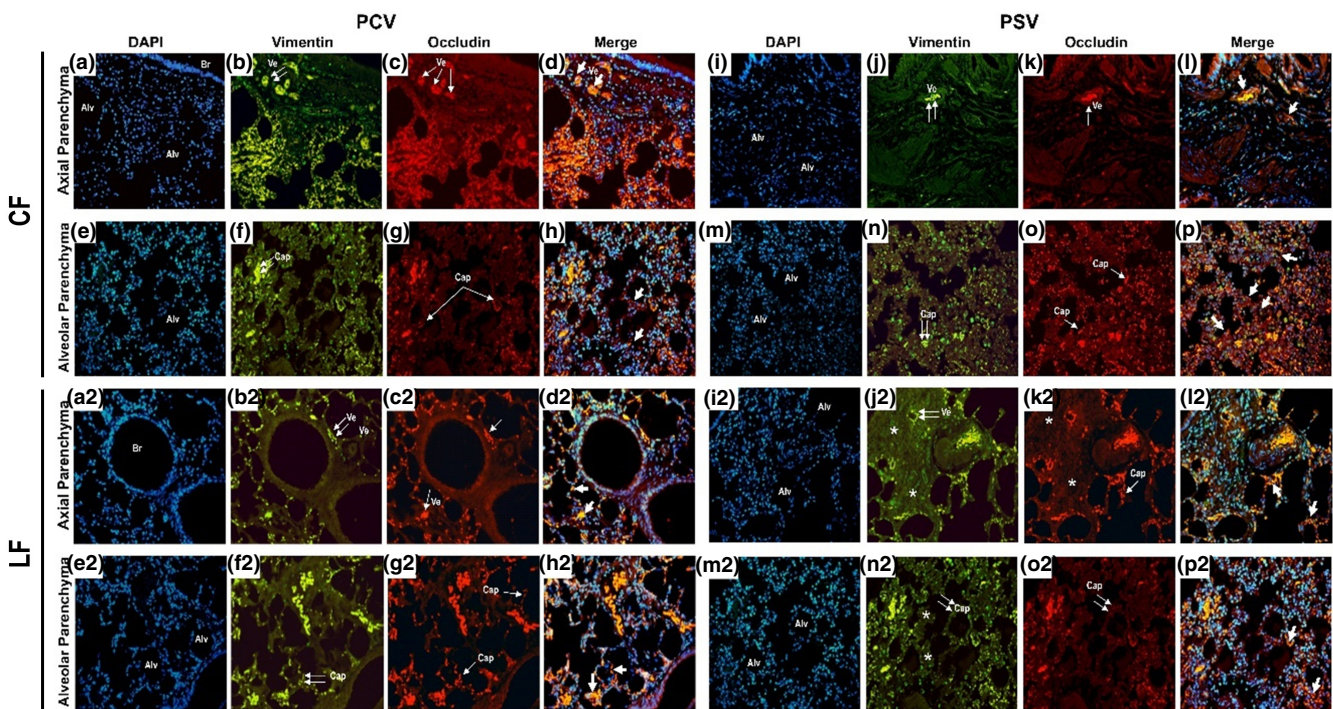
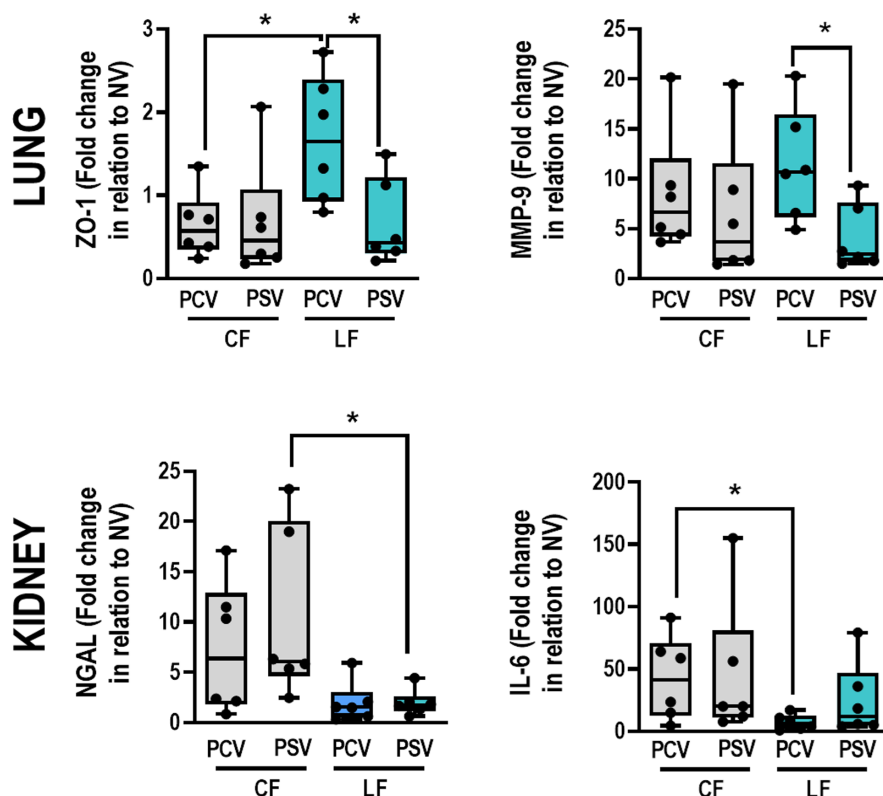


**FIGURE 3** Immunofluorescence of occludin and vimentin. Histologic sections ( $\times 400$ ) of the axial and alveolar staining for immunofluorescence to occludin and vimentin divided by groups (CF-PCV, CF-PSV, LF-PCV, and LF-PSV). The arrows indicate the endothelial cells of the bronchiolar and alveolar capillaries expressing occludin [nuclei in blue, 4',6-diamidino-2-phenylindole (DAPI); connective tissue in green; vimentin; bronchiolar vessels and alveolar capillaries in red; occludin and colocalization, blue-orange-red]. (a) DAPI (nuclei in blue) in axial parenchyma in CF-PCV. (b,f) Vimentin in axial parenchyma in CF-PCV. (d) Merge of DAPI, vimentin and occludin in axial parenchyma in CF-PCV. (e) DAPI (nuclei in blue) in alveolar parenchyma in CF-PCV. (f) Vimentin in alveolar parenchyma in CF-PCV. (h) Merge of DAPI, vimentin and occludin in alveolar parenchyma in CF-PCV. (i) DAPI (nuclei in blue) in axial parenchyma in CF-PSV. (j) Vimentin in axial parenchyma in CF-PSV. (l) Merge of DAPI, vimentin and occludin in axial parenchyma in CF-PSV. (m) DAPI (nuclei in blue) in alveolar parenchyma in CF-PSV. (n) Vimentin in alveolar parenchyma in CF-PSV. (p) Merge of DAPI, vimentin and occludin in alveolar parenchyma in CF-PSV. The CF-PCV parenchyma (C and G) presents intense red birefringence of occludin in dilated lymphatics and blood vessels around the bronchiolar mucosa and along the capillary alveoli (simple white arrows). CF-PSV and LF-PCV (K, O, C2, and G2) present a similar pattern of birefringence for occludin (red) in endothelial cells of the lymphatics and blood vessels (double white arrows), as well as along capillaries of the alveolar septa (single white arrows). In contrast, LF-PSV (K2 and O2) has almost no birefringence of occludin in the endothelium of the lymphatics and blood vessels, as well as along capillaries of the alveolar septa, with prominent oedema in this group (\*). Br, bronchioles; Alv, alveoli; Ve, blood vessels; Cap, capillaries. White double arrows, connective tissue around bronchiolar vessels and alveolar capillaries. Simple white arrows, expression of occludin by endothelial cells of bronchiolar vessels and alveolar capillaries; white arrowhead, colocalization of vimentin and occludin; \*, peribronchiolar and alveolar cuff.



**FIGURE 4** Molecular biology of lung and kidney. Gene expression of ZO-1 and MMP-9 in lung tissue; and KIM-1, NGAL, and IL-6 in kidney tissue. Boxplots represent the median and interquartile range of 6 animals per group. Comparisons were done by Kruskal–Wallis test followed by Dunn’s multiple comparisons test ( $p < 0.05$ ). CF, conservative fluid therapy; IL-6, interleukin-6; KIM-1, kidney injury molecule 1; LF, liberal fluid therapy; MMP-9, metalloproteinase-9; NGAL, neutrophilic gelatinase-associated lipocalin; PCV, pressure-controlled ventilation; PSV, pressure-support ventilation; ZO-1, zona occludens-1; \*, depicting the differences between groups ( $p < 0.05$ ).



not produce severe hemodynamic instability (Famous et al., 2017). Similar results have been shown previously by our group (Magalhães et al., 2018; Moraes et al., 2014, 2018; Rocha et al., 2021; Saddy et al., 2013). We defined the LF rate as four times the CF rate because there is a lack of consensus on what a “liberal” fluid strategy means in clinical practice (Rahbari et al., 2009). Nevertheless, the difference between the CF and LF infusion rates was close to that in many other studies (Holte et al., 2007; Kotlińska-Hasiec et al., 2017; Lobo et al., 2011; Shin et al., 2018). Even though  $CO_{LV}$  and MAP were similar between the groups and time points, the fluid rate difference was sufficient to create two different hemodynamic profiles as demonstrated by lower  $SVV_{LV}$  and VCCI at  $T_{60}$  in the LF-PCV group. These results suggest a fluid overload (corresponding to Frank-Starling’s curve plateau) that could potentially increase the hydrostatic pressure in pulmonary capillaries. All groups were successfully ventilated under protective  $V_T$  ( $\approx 6$  ml/kg) and had similar alveolar heterogeneity indexes as previously reported (Pinto et al., 2020).

Although perivascular edema was positively correlated with higher fluid infusion rates (i.e., higher in the LF groups regardless of the ventilatory strategies), edema in axial and alveolar lung parenchyma yielded higher cumulative DAD scores in the LF-PSV group. The LF-PSV group had higher edema scores than reported in previous studies not combining LFs and spontaneous breathing (Magalhães et al., 2018; Moraes et al., 2018; Pinto et al., 2020; Silva et al., 2018). We can explain the increase in axial and alveolar edema and

ultimately the DAD score in the LF-PSV group as follows: (1) under an LF strategy, an increase in hydrostatic capillary pressure and filtration is expected, mainly at increased lung permeability, as caused by LPS (Pugin et al., 1999; Ware & Matthay, 2000); (2) during PSV, transpulmonary pressure is determined by increased airway pressure and decreased pleural pressure, leading to tensile stress (Bellani et al., 2016; Saddy et al., 2014), which in turn, may stretch alveolar units through repetitive movements; and (3) edema may increase further if tight junction connections, which are constitutive in epithelial and endothelial structural cells, are lost during the stretch movements produced by tensile stress in PSV (Cavanaugh Jr et al., 2001). In addition, the level of neuromuscular drive ( $Poes_{0.1}$ ) in CF or LF groups during PSV was similar to other studies in small animals with ALI (da Cruz et al., 2021). We hypothesize that injury in tight junctions has a mechanistic relationship with fluid overload because expression of occludin was lower in the LF-PSV group and negatively correlated with edema with lower birefringence for claudin-4. Similar behavior was not observed with the CF strategy in combination with pressure support ventilation. This suggests that the application of pressure support ventilation during early hemodynamic resuscitation may worsen lung injury.

LF-PSV had lower expression of ZO1 than LF-PCV, suggesting less tight junction recovery and higher cell proliferation with suppression of apoptosis (Meng et al., 2020; Ogata-Suetsugu et al., 2017). Lower MMP-9 gene expression with LF-PSV than with LF-PCV has already been described

in a similar model of acute respiratory distress syndrome receiving approximately 10 ml/kg/h of fluids (Pinto et al., 2020), a difference not observed under a CF strategy.

Kidney histology indicates that both CF and LF were not associated with increased injury. It is possible that the AKI score and brush border analysis revealed almost no impact because of the short time span of the intervention. Kidney gene expression was similar between the groups, although in a post-hoc analysis, both LF-PCV and LF-PSV groups had significantly lower expression of NGAL and IL-6 than in the CF groups. This suggests that the CF strategy may be associated with some degree of kidney injury, although we did not analyze urine or blood markers of kidney function.

#### 4.1 | Limitations

The study has some limitations to be addressed. First, the results apply to this specific model of ALI and cannot be directly extrapolated to the clinical scenario. However, as extensively discussed previously for LPS models (Cardinal-Fernández et al., 2017; Matute-Bello et al., 2008), the DAD scores presented here confirm ALI just as in previous studies. The histologic features better represent mild lung injury from LPS instillations in small animals (Matute-Bello et al., 2011). Second, the LF rates used here were relatively high; nevertheless, studies show similar fluid rates in clinical scenarios (Holte et al., 2007; Kotlińska-Hasiec et al., 2017; Lobo et al., 2011; Shin et al., 2018). Furthermore, we aimed to investigate groups with extreme and different fluid strategies. Third, due to the study design, only the PCV group required neuromuscular blockade, and these drugs may reduce inflammatory responses in the setting of ALI (Forel et al., 2006). Fourth, whether a higher PEEP strategy would protect from the effects of pressure support ventilation and LF management on pulmonary edema remains unknown. Fifth, although the time under mechanical ventilation is relatively short, it should be normalized to the metabolism of small mammals whereby 1 rat hour approximates 27 human hours (Agoston, 2017), and specifically to VILI progression, it should be normalized to breathing frequency (6- to 7-fold higher in rats than humans). Nevertheless, the 1-h experiment was time enough to observe decrements in constitutive proteins at the alveolar-capillary membrane and changes in gene expression.

#### 5 | CONCLUSIONS

CF compared with LF during pressure support ventilation yielded less lung epithelial cell damage in the current

model of ALI. However, LF compared with conservative fluid resulted in less kidney injury markers, regardless of the ventilatory strategy.

#### AUTHOR CONTRIBUTIONS

This study was conducted at the Pulmonary Investigation Laboratory in Institute of Biophysics Carlos Chagas Filho in Federal University of Rio de Janeiro. Eduardo Butturini de Carvalho, Marcelo Gama de Abreu, Nathane Santanna Felix, Paolo Pelosi, Patrícia Rieken Macêdo Rocco, and Pedro Leme Silva were involved in the conception or design of the work; Eduardo Butturini de Carvalho, Ana Carolina Fernandes Fonseca, Raquel Ferreira Magalhães, Eliete Ferreira Pinto, Cynthia dos Santos Samary, Mariana Alves Antunes, Camila Machado Baldavira, Lizandre Keren Ramos da Silveira, Walcy Rosolia Teodoro, Vera Luiza Capelozzi, and Pedro Leme Silva took part in the acquisition, analysis or interpretation of data; Eduardo Butturini de Carvalho, Marcelo Gama de Abreu, Nathane Santanna Felix, Paolo Pelosi, Patrícia Rieken Macêdo Rocco, and Pedro Leme Silva drafted the work or revised it critically for important intellectual content. All authors approved the final version of the manuscript, agree to be accountable for all aspects of the work, ensuring that questions related to the accuracy or integrity of any part of the work are appropriately investigated and resolved. All persons designated as authors qualify for authorship, and all those who qualify for authorship are listed.

#### ACKNOWLEDGMENTS

The authors express their gratitude to the following people from the Laboratory of Pulmonary Investigation, Carlos Chagas Filho Biophysics Institute, Federal University of Rio de Janeiro, Rio de Janeiro, Brazil: Andre Benedito da Silva, BSc, for animal care; Arlete Fernandes, BSc, for her help with microscopy; Maíra Rezende Lima, MSc, for her assistance with molecular biology analysis; and to Moira Elizabeth Shottler, mBA, Rio de Janeiro, Brazil, and Filipe Vasconcellos, São Paulo, Brazil for editing assistance.

#### FUNDING INFORMATION

This study was supported by the Brazilian Council for Scientific and Technological Development (CNPq; 483005/2020-6), the Rio de Janeiro State Research Foundation (FAPERJ), São Paulo Research Foundation (FAPESP; 2018/20403-6, 2019/12151-367 0), and Coordination for the Improvement of Higher Education Personnel (CAPES) (CAPES; Finance Code 001), and the Department of Science and Technology - Brazilian Ministry of Health (DECIT/MS).

## CONFLICT OF INTEREST

The authors declare no competing interests.

## ORCID

Pedro Leme Silva  <https://orcid.org/0000-0001-5838-4949>

[org/0000-0001-5838-4949](https://orcid.org/0000-0001-5838-4949)

## REFERENCES

- Agoston, D. V. (2017). How to translate time? The temporal aspect of human and rodent biology. *Frontiers in Neurology*, *8*, 92.
- Akamine, R., Yamamoto, T., Watanabe, M., Yamazaki, N., Kataoka, M., Ishikawa, M., Ooie, T., Baba, Y., & Shinohara, Y. (2007). Usefulness of the 5' region of the cDNA encoding acidic ribosomal phosphoprotein P0 conserved among rats, mice, and humans as a standard probe for gene expression analysis in different tissues and animal species. *Journal of Biochemical and Biophysical Methods*, *70*, 481–486.
- Bachofen, H., Schurch, S., Urbinelli, M., & Weibel, E. R. (1987). Relations among alveolar surface tension, surface area, volume, and recoil pressure. *Journal of Applied Physiology*, *62*, 1878–1887.
- Balancin, M. L., Teodoro, W. R., Baldavira, C. M., Prieto, T. G., Farhat, C., Velosa, A. P., da Costa Souza, P., Yaegashi, L. B., Ab'Saber, A. M., & Takagaki, T. Y. (2020). Different histological patterns of type-V collagen levels confer a matrices-privileged tissue microenvironment for invasion in malignant tumors with prognostic value. *Pathology, Research and Practice*, *216*, 153277.
- Balancin, M. L., Teodoro, W. R., Farhat, C., de Miranda, T. J., Assato, A. K., de Souza Silva, N. A., Velosa, A. P., Falzoni, R., Ab'Saber, A. M., & Roden, A. C. (2020). An integrative histopathologic clustering model based on immuno-matrix elements to predict the risk of death in malignant mesothelioma. *Cancer Medicine*, *9*, 4836–4849.
- Bateman, R. M., Sharpe, M. D., Jagger, J. E., Ellis, C. G., Solé-Violán, J., López-Rodríguez, M., Herrera-Ramos, E., Ruiz-Hernández, J., Borderías, L., Horcajada, J., González-Quevedo, N., Rajas, O., Briones, M., Rodríguez de Castro, F., Rodríguez Gallego, C., Esen, F., Orhun, G., Ergin Ozcan, P., Senturk, E., ... Prandi, E. (2016). 36th international symposium on intensive care and emergency medicine: Brussels, Belgium. 15–18 March 2016. *Critical Care*, *20*, 94.
- Baydur, A., Behrakis, P. K., Zin, W. A., Jaeger, M., & Milic-Emili, J. (1982). A simple method for assessing the validity of the esophageal balloon technique. *The American Review of Respiratory Disease*, *126*, 788–791.
- Bellani, G., Grasselli, G., Tegaglia-Droghi, M., Mauri, T., Coppadoro, A., Brochard, L., & Pesenti, A. (2016). Do spontaneous and mechanical breathing have similar effects on average transpulmonary and alveolar pressure? A clinical crossover study. *Critical Care*, *20*, 1–10.
- Cardinal-Fernández, P., Lorente, J. A., Ballén-Barragán, A., & Matute-Bello, G. (2017). Acute respiratory distress syndrome and diffuse alveolar damage. New insights on a complex relationship. *Annals of the American Thoracic Society*, *14*, 844–850.
- Cavalcanti, V., Santos, C. L., Samary, C. S., Araújo, M. N., Heil, L. B. B., Morales, M. M., Silva, P. L., Pelosi, P., Fernandes, F. C., Villela, N., & Rocco, P. R. M. (2014). Effects of short-term propofol and dexmedetomidine on pulmonary morphofunction and biological markers in experimental mild acute lung injury. *Respiratory Physiology & Neurobiology*, *203*, 45–50.
- Cavanaugh, K. J., Jr., Oswari, J., & Margulies, S. S. (2001). Role of stretch on tight junction structure in alveolar epithelial cells. *American Journal of Respiratory Cell and Molecular Biology*, *25*, 584–591.
- Cruz, F. F., Ball, L., Rocco, P. R. M., & Pelosi, P. (2018). Ventilator-induced lung injury during controlled ventilation in patients with acute respiratory distress syndrome: Less is probably better. *Expert Review of Respiratory Medicine*, *12*, 403–414.
- da Cruz, D. G., de Magalhaes, R. F., Padilha, G. A., da Silva, M. C., Braga, C. L., Silva, A. R., Goncalves de Albuquerque, C. F., Capelozzi, V. L., Samary, C. S., & Pelosi, P. (2021). Impact of positive biphasic pressure during low and high inspiratory efforts in *Pseudomonas aeruginosa*-induced pneumonia. *PLoS One*, *16*, e0246891.
- Elliott, M. W., Mulvey, D. A., Green, M., & Moxham, J. (1993). An evaluation of P0.1 measured in mouth and oesophagus, during carbon dioxide rebreathing in COPD. *The European Respiratory Journal*, *6*, 1055–1059.
- Famous, K. R., Delucchi, K., Ware, L. B., Kangelaris, K. N., Liu, K. D., Thompson, B. T., & Calfee, C. S. (2017). Acute respiratory distress syndrome subphenotypes respond differently to randomized fluid management strategy. *American Journal of Respiratory and Critical Care Medicine*, *195*, 331–338.
- Forel, J.-M., Roch, A., Marin, V., Michelet, P., Demory, D., Blache, J.-L., Perrin, G., Gannier, M., Bongrand, P., & Papazian, L. (2006). Neuromuscular blocking agents decrease inflammatory response in patients presenting with acute respiratory distress syndrome. *Critical Care Medicine*, *34*, 2749–2757.
- Gattinoni, L., Protti, A., Caironi, P., & Carlesso, E. (2010). Ventilator-induced lung injury: The anatomical and physiological framework. *Critical Care Medicine*, *38*(10 Suppl), S539–S548.
- Holte, K., Hahn, R. G., Ravn, L., Bertelsen, K. G., Hansen, S., & Kehlet, H. (2007). Influence of “liberal” versus “restrictive” intraoperative fluid administration on elimination of a postoperative fluid load. *Anesthesiology*, *106*, 75–79.
- Hsia, C. C. W., Hyde, D. M., Ochs, M., & Weibel, E. R. (2010). An official research policy statement of the American Thoracic Society/European Respiratory Society: Standards for quantitative assessment of lung structure. *American Journal of Respiratory and Critical Care Medicine*, *81*, 394–418.
- Huppert, L. A., Matthay, M. A., & Ware, L. B. (2019). Pathogenesis of acute respiratory distress syndrome. *Seminars in Respiratory and Critical Care Medicine*, *40*, 31–39.
- Hüter, L., Simon, T.-P., Weinmann, L., Schuerholz, T., Reinhart, K., Wolf, G., Amann, K. U., & Marx, G. (2009). Hydroxyethylstarch impairs renal function and induces interstitial proliferation, macrophage infiltration and tubular damage in an isolated renal perfusion model. *Critical Care*, *13*, 1–9.
- Kiss, T., Silva, P. L., Huhle, R., Moraes, L., Santos, R. S., Felix, N. S., Santos, C. L., Morales, M. M., Capelozzi, V. L., Kasper, M., Pelosi, P., Gama de Abreu, M., & Rocco, P. R. M. (2016). Comparison of different degrees of variability in tidal volume to prevent deterioration of respiratory system elastance in experimental acute lung inflammation. *British Journal of Anaesthesia*, *116*, 708–715.
- Kotlińska-Hasiec, E., Rutyna, R. R., Rzecki, Z., Czarko-Wicha, K., Gagała, J., Pawlik, P., Załuska, A., Jaroszyński, A., Załuska,



- W., & Dąbrowski, W. (2017). The effect of crystalloid infusion on body water content and intra-abdominal pressure in patients undergoing orthopedic surgery under spinal anesthesia. *Advances in Clinical and Experimental Medicine*, *26*, 1189–1196.
- Lang, R. M., Badano, L. P., Victor, M. A., Afilalo, J., Armstrong, A., Ernande, L., Flachskampf, F. A., Foster, E., Goldstein, S. A., Kuznetsova, T., Lancellotti, P., Muraru, D., Picard, M. H., Retzschel, E. R., Rudski, L., Spencer, K. T., Tsang, W., & Voigt, J. U. (2015). Recommendations for cardiac chamber quantification by echocardiography in adults: An update from the American Society of Echocardiography and the European Association of Cardiovascular Imaging. *Journal of the American Society of Echocardiography*, *28*, 1–39.e14.
- Lobo, S. M., Ronchi, L. S., Oliveira, N. E., Brandão, P. G., Froes, A., Cunrath, G. S., Nishiyama, K. G., Netinho, J. G., & Lobo, F. R. (2011). Restrictive strategy of intraoperative fluid maintenance during optimization of oxygen delivery decreases major complications after high-risk surgery. *Critical Care*, *15*, R226.
- Magalhães, P. A. F., De Padilha, G. A., Moraes, L., Santos, C. L., De Maia, L. A., Braga, C. L., Duarte, M. D. C. M. B., Andrade, L. B., Schanaider, A., Capellozzi, V. L., Huhle, R., Gama De Abreu, M., Pelosi, P., Rocco, P. R. M., & Silva, P. L. (2018). Effects of pressure support ventilation on ventilator-induced lung injury in mild acute respiratory distress syndrome depend on level of positive end-expiratory pressure. *European Journal of Anaesthesiology*, *35*, 298–306.
- Marini, J. J., & Rocco, P. R. M. (2020). Which component of mechanical power is most important in causing VILI? *Critical Care*, *24*, 39.
- Matute-Bello, G., Downey, G., Moore, B. B., Groshong, S. D., Matthay, M. A., Slutsky, A. S., & Kuebler, W. M. (2011). An official American Thoracic Society workshop report: Features and measurements of experimental acute lung injury in animals. *American Journal of Respiratory Cell and Molecular Biology*, *44*, 725–738.
- Matute-Bello, G., Frevert, C. W., & Martin, T. R. (2008). Animal models of acute lung injury. *American Journal of Physiology. Lung Cellular and Molecular Physiology*, *295*, L379–L399.
- Mekontso Dessap, A., Boissier, F., Charron, C., Bégot, E., Repessé, X., Legras, A., Brun-Buisson, C., Vignon, P., & Vieillard-Baron, A. (2016). Acute cor pulmonale during protective ventilation for acute respiratory distress syndrome: Prevalence, predictors, and clinical impact. *Intensive Care Medicine*, *42*, 862–870.
- Meng, C., Wang, S., Wang, X., Lv, J., Zeng, W., Chang, R., Li, Q., & Wang, X. (2020). Amphiregulin inhibits TNF- $\alpha$ -induced alveolar epithelial cell death through EGFR signaling pathway. *Biomedicine & Pharmacotherapy*, *125*, 109995.
- Moraes, L., Santos, C. L., Santos, R. S., Cruz, F. F., Saddy, F., Morales, M. M., Capellozzi, V. L., Silva, P. L., de Abreu, M. G., & Garcia, C. S. N. B. (2014). Effects of sigh during pressure control and pressure support ventilation in pulmonary and extrapulmonary mild acute lung injury. *Critical Care*, *18*, 1–13.
- Moraes, L., Silva, P. L., Thompson, A., Santos, C. L., Santos, R. S., Fernandes, M. V. S., Morales, M. M., Martins, V., Capellozzi, V. L., de Abreu, M. G., Pelosi, P., & Rocco, P. R. M. (2018). Impact of different tidal volume levels at low mechanical power on ventilator-induced lung injury in rats. *Frontiers in Physiology*, *9*, 318.
- Ogata-Suetsugu, S., Yanagihara, T., Hamada, N., Ikeda-Harada, C., Yokoyama, T., Suzuki, K., Kawaguchi, T., Maeyama, T., Kuwano, K., & Nakanishi, Y. (2017). Amphiregulin suppresses epithelial cell apoptosis in lipopolysaccharide-induced lung injury in mice. *Biochemical and Biophysical Research Communications*, *484*, 422–428.
- Parameswaran, H., Majumdar, A., Ito, S., Alencar, A. M., & Suki, B. (2006). Quantitative characterization of airspace enlargement in emphysema. *Journal of Applied Physiology*, *100*, 186–193.
- Percie du Sert, N., Hurst, V., Ahluwalia, A., Alam, S., Avey, M. T., Baker, M., Browne, W. J., Clark, A., Cuthill, I. C., & Dirnagl, U. (2020). The ARRIVE guidelines 2.0: Updated guidelines for reporting animal research. *Journal of Cerebral Blood Flow and Metabolism*, *40*, 1769–1777.
- Pinto, E. F., Santos, R. S., Antunes, M. A., Maia, L. A., Padilha, G. A., de A Machado, J., Carvalho, A. C. F., Fernandes, M. V. S., Capellozzi, V. L., & de Abreu, M. G. (2020). Static and dynamic transpulmonary driving pressures affect lung and diaphragm injury during pressure-controlled versus pressure-support ventilation in experimental mild lung injury in rats. *Anesthesiology*, *132*, 307–320.
- Pugin, J., Verghese, G., Widmer, M.-C., & Matthay, M. A. (1999). The alveolar space is the site of intense inflammatory and profibrotic reactions in the early phase of acute respiratory distress syndrome. *Critical Care Medicine*, *27*, 304–312.
- Rahbari, N. N., Zimmermann, J. B., Schmidt, T., Koch, M., Weigand, M. A., & Weitz, J. (2009). Meta-analysis of standard, restrictive and supplemental fluid administration in colorectal surgery. *The British Journal of Surgery*, *96*, 331–341.
- Roan, E., & Waters, C. M. (2011). What do we know about mechanical strain in lung alveoli? *American Journal of Physiology. Lung Cellular and Molecular Physiology*, *301*, L625–L635.
- Rocha, N. N., Samary, C. S., Antunes, M. A., Oliveira, M. V., Hemerly, M. R., Santos, P. S., Capellozzi, V. L., Cruz, F. F., Marini, J. J., & Silva, P. L. (2021). The impact of fluid status and decremental PEEP strategy on cardiac function and lung and kidney damage in mild-moderate experimental acute respiratory distress syndrome. *Respiratory Research*, *22*, 1–12.
- Saddy, F., Moraes, L., Santos, C. L., Oliveira, G. P., Cruz, F. F., Morales, M. M., Capellozzi, V. L., de Abreu, M. G., Baez Garcia, C. S. N., Pelosi, P., & Macêdo Rocco, P. R. (2013). Biphasic positive airway pressure minimizes biological impact on lung tissue in mild acute lung injury independent of etiology. *Critical Care*, *17*, R228.
- Saddy, F., Oliveira, G. P., Garcia, C. S. N. B., Nardelli, L. M., Rzezinski, A. F., Ornellas, D. S., Morales, M. M., Capellozzi, V. L., Pelosi, P., & Rocco, P. R. M. (2010). Assisted ventilation modes reduce the expression of lung inflammatory and fibrogenic mediators in a model of mild acute lung injury. *Intensive Care Medicine*, *36*, 1417–1426.
- Saddy, F., Sutherasan, Y., Rocco, P. R. M., & Pelosi, P. (2014). Ventilator-associated lung injury during assisted mechanical ventilation. *Seminars in Respiratory and Critical Care Medicine*, *35*, 409–417.
- Santiago, V. R., Rzezinski, A. F., Nardelli, L. M., Silva, J. D., Garcia, C. S. N. B., Maron-Gutierrez, T., Ornellas, D. S., Morales, M. M., Capellozzi, V. L., & Marini, J. (2010). Recruitment maneuver in experimental acute lung injury: The role of alveolar collapse and edema. *Critical Care Medicine*, *38*, 2207–2214.
- Santos, C. L., Santos, R. S., Moraes, L., Samary, C. S., Felix, N. S., Silva, J. D., Morales, M. M., Huhle, R., Abreu, M. G., Schanaider, A., Silva, P. L., Pelosi, P., & Rocco, P. R. M. (2017). Effects of

- pressure support and pressurecontrolled ventilation on lung damage in a model of mild extrapulmonary acute lung injury with intra-abdominal hypertension. *PLoS One*, *12*, e0178207.
- Shin, C. H., Long, D. R., McLean, D., Grabitz, S. D., Ladha, K., Timm, F. P., Thevathasan, T., Pieretti, A., Ferrone, C., Hoeft, A., Scheeren, T. W. L., Thompson, B. T., Kurth, T., & Eikermann, M. (2018). Effects of intraoperative fluid management on postoperative outcomes: A hospital registry study. *Annals of Surgery*, *267*, 1084–1092.
- Silva, P. L., Ball, L., Rocco, P. R. M., & Pelosi, P. (2022). Physiological and pathophysiological consequences of mechanical ventilation. *Seminars in Respiratory and Critical Care Medicine*, *43*, 321–334. <https://doi.org/10.1055/s-0042-1744447>
- Silva, P. L., Cruz, F. F., dos Santos Samary, C., Moraes, L., de Magalhães, R. F., Fernandes, M. V., de S Bose, R., Pelegati, V. B., Carvalho, H. F., & Capelozzi, V. L. (2018). Biological response to time-controlled adaptive ventilation depends on acute respiratory distress syndrome etiology. *Critical Care Medicine*, *46*, e609–e617.
- Silva, P. L., & de Abreu, M. G. (2018). Regional distribution of transpulmonary pressure. *Annals of Translational Medicine*, *6*, 385.
- Silva, P. L., Moraes, L., Santos, R. S., Samary, C., Ramos, M. B. A., Santos, C. L., Morales, M. M., Capelozzi, V. L., Garcia, C. S. N. B., De Abreu, M. G., Pelosi, P., Marini, J. J., & Rocco, P. R. M. (2013). Recruitment maneuvers modulate epithelial and endothelial cell response according to acute lung injury etiology. *Critical Care Medicine*, *41*, e256–e265.
- Tschumperlin, D. J., Oswari, J., & Margulies, A. S. S. (2000). Deformation-induced injury of alveolar epithelial cells. *American Journal of Respiratory and Critical Care Medicine*, *162*, 357–362.
- Uhlir, C., Silva, P. L., Ornellas, D., Santos, R. S., Miranda, P. J., Spieth, P. M., Kiss, T., Kasper, M., Wiedemann, B., Koch, T., Morales, M. M., Pelosi, P., De Abreu, M. G., & Rocco, P. R. M. (2014). The effects of salbutamol on epithelial ion channels depend on the etiology of acute respiratory distress syndrome but not the route of administration. *Respiratory Research*, *15*, 56.
- van Haren, F., Pham, T., Brochard, L., Bellani, G., Laffey, J., Dres, M., Fan, E., Goligher, E. C., Heunks, L., Lynch, J., Wrigge, H., McAuley, D., & Large observational study to UNDERstand the Global impact of Severe Acute respiratory FailurE (LUNG SAFE) Investigators. (2019). Spontaneous breathing in early acute respiratory distress syndrome: Insights from the large observational study to UNDERstand the global impact of severe acute respiratory FailurE study. *Critical Care Medicine*, *47*, 229–238.
- Vieillard-Baron, A., Matthay, M., Teboul, J. L., Bein, T., Schultz, M., Magder, S., & Marini, J. J. (2016). Experts' opinion on management of hemodynamics in ARDS patients: Focus on the effects of mechanical ventilation. *Intensive Care Medicine*, *42*, 739–749.
- Ware, L. B., & Matthay, M. A. (2000). The acute respiratory distress syndrome. *The New England Journal of Medicine*, *342*, 1334–1349.
- Watson, L. E., Sheth, M., Denyer, R. F., & Dostal, D. E. (2004). Baseline echocardiographic values for adult male rats. *Journal of the American Society of Echocardiography*, *17*, 161–167.
- Wierzchon, C. G. R. S., Padilha, G., Rocha, N. N., Huhle, R., Coelho, M. S., Santos, C. L., Santos, R. S., Samary, C. S., Silvino, F. R. G., Pelosi, P., de Abreu, M. G., Rocco, P. R. M., & Silva, P. L. (2017). Variability in tidal volume affects lung and cardiovascular function differentially in a rat model of experimental emphysema. *Frontiers in Physiology*, *8*, 1071.
- Yoshida, T., Fujino, Y., Amato, M. B. P., & Kavanagh, B. P. (2017). Fifty years of research in ARDS. Spontaneous breathing during mechanical ventilation risks, mechanisms, and management. *American Journal of Respiratory and Critical Care Medicine*, *195*, 985–992.

## SUPPORTING INFORMATION

Additional supporting information can be found online in the Supporting Information section at the end of this article.

**How to cite this article:** de Carvalho, E. B., Fonseca, A. C. F., Magalhães, R. F., Pinto, E. F., Samary, C. d. S., Antunes, M. A., Baldavira, C. M., da Silveira, L. K. R., Teodoro, W. R., de Abreu, M. G., Capelozzi, V. L., Felix, N. S., Pelosi, P., Rocco, P. R. M., & Silva, P. L. (2022). Effects of different fluid management on lung and kidney during pressure-controlled and pressure-support ventilation in experimental acute lung injury. *Physiological Reports*, *10*, e15429. <https://doi.org/10.14814/phy2.15429>